Earth and Planetary Science Letters 594 (2022) 117695

Contents lists available at ScienceDirect

Earth and Planetary Science Letters

www.elsevier.com/locate/epsl

Fluid processes in the early Earth and the growth of continents

Michael I.H. Hartnady [a,*,1], Tim E. Johnson [a], Simon Schorn [b], R. Hugh Smithies [c,1], Christopher L. Kirkland [a,1], Stephen H. Richardson [d]

[a] School of Earth and Planetary Science, Curtin University, Perth, Australia
[b] NAWI Graz Geocenter, University of Graz, Universitätsplatz 2, Graz, Austria
[c] Geological Survey of Western Australia, 100 Plain Street, East Perth, WA, Australia
[d] Department of Geological Sciences, University of Cape Town, Rondebosch, South Africa

ARTICLE INFO

Article history:
Received 1 April 2022
Received in revised form 14 June 2022
Accepted 23 June 2022
Available online 25 July 2022
Editor: F. Moynier

Dataset link: http://www.metamorph.geo.uni-mainz.de/thermocalc

Keywords:
fluid processes
komatiite
tonalite-trondhjemite-granodiorite (TTG)
Archaean crustal evolution

ABSTRACT

Water is an essential ingredient in transforming primitive mantle-derived (mafic) rocks into buoyant (felsic) continental crust, thereby driving the irreversible differentiation of Earth's lithosphere. The occurrence in Archaean cratons of sodic granites of the tonalite–trondhjemite–granodiorite (TTG) series, high-MgO variolitic basalts, high-Mg diorites (sanukitoids) and diamonds with harzburgitic inclusion assemblages, all require the presence of hydrous fluids in Earth's deep crust and upper (lithospheric) mantle since at least the Paleoarchaean (3.6–3.2 billion years ago). However, despite its importance, where and how water was stored in Archaean crust, and how some water was transported into the upper mantle, are poorly understood. Here, we investigate Archaean crustal fluid budgets through calculated phase equilibria for three protolith compositions — a low-MgO mafic (basaltic) composition, a high-MgO (picritic) composition and an ultrahigh-MgO ultramafic (komatiitic) composition — that are representative of mafic to ultramafic magmatic rocks in Archaean greenstone belts. We show that the mode and stability of hydrous minerals, in particular chlorite, is positively correlated with protolith MgO content, such that high-MgO basalts can store up to twice the amount of crystal-bound H_2O than low-MgO basalts. Importantly, ultrahigh-MgO rocks such as komatiite can store four times as much H_2O, most of which is retained until temperatures exceeding 700 °C. Warmer geotherms in the early Archaean favoured dehydration of hydrated high-MgO and ultramafic rocks in the deep crust, leading to hydration and/or fluid-fluxed melting of overlying basaltic rocks to produce 'high-pressure' TTG magmas. Burial of Archaean mafic–ultramafic crust along cooler geotherms resulted in dehydration of ultramafic material within the lithospheric mantle, providing the source of enriched Archaean basalt that was parental to large volumes of ancient TTG-dominated continental crust.

1. Introduction

Much of Earth's oldest continental crust consists of deformed and metamorphosed felsic magmatic rocks of the tonalite–trondhjemite–granodiorite (TTG) series, sodic granitoids with high SiO_2 (~65–75 wt%) and Al_2O_3 (~15 wt%) contents, and high La/Yb, Sr/Y and Na_2O/K_2O ratios (Smithies et al., 2009; Moyen, 2011). Although it is widely accepted that TTG magmas were produced by partial melting of hydrated basaltic sources (i.e. amphibolite, Barker and Arth, 1976), the geodynamic setting(s) in which they formed is debated (Kleinhanns et al., 2003; Bédard, 2006; Moyen, 2011; Johnson et al., 2017; Pourteau et al., 2020; Smithies et al., 2021).

Variations in the trace element compositions of TTG are commonly argued to reflect the pressure of melt generation (Moyen, 2011). Most TTGs were likely produced by fluid-absent anatexis ('dehydration melting') of garnet-bearing amphibolite in shallow subduction systems or the deeper levels of thick Archean primary (oceanic) crust (Johnson et al., 2017). However, around 20% of TTG have elevated Sr, Al_2O_3 and Na_2O contents, which some think reflects partial melting of deeply-subducted oceanic crust at pressures exceeding plagioclase stability (>2.5 GPa, Moyen and Stevens, 2006). By contrast, others have argued that these 'high-*P*' signatures may indicate either hydrous-fluid-fluxed ('wet') melting of amphibolite (Pourteau et al., 2020) or fractional crystallisation of hydrous mafic–intermediate magmas at shallow or deep crustal

* Corresponding author.
E-mail address: Michael.hartnady@curtin.edu.au (M.I.H. Hartnady).
[1] Timescales of Mineral Systems Group.

https://doi.org/10.1016/j.epsl.2022.117695

levels (Kleinhanns et al., 2003; Smithies et al., 2021; Liou et al., 2022)

Regardless of the tectonic setting, a critical role for fluids is implicated in nearly all models of TTG formation (André et al., 2019, 2022; Smithies et al., 2021). Seawater is an obvious source of this water, particularly given that a global ocean likely covered most of Earth's surface in the early Archaean (Bindeman et al., 2018). Moreover, silicification during seafloor alteration likely played an important role in increasing the SiO_2 content, and thereby the potential melt fertility, of the hydrated mafic (amphibolite) protoliths (Stuck and Diener, 2017, André et al., 2019, 2022).

In addition to near-surface environments, various lines of evidence indicate the existence of a deep fluid reservoir in the early Earth (Byerly et al., 2017; Sobolev et al., 2019; Smithies et al., 2021). Many greenstone sequences contain enriched and 'boninite-like' rocks derived from depleted mantle peridotite that interacted with trace-element-enriched fluids released from recycled supracrustal material (Smithies, 2002). Many Archaean cratons also preserve high-Mg basaltic rocks with variolitic textures and trace-element enriched high-Mg porphyritic diorite (i.e. sanukitoid), both of which are believed to originate via fluid-fluxed melting of lithospheric mantle peridotite (Shirey and Hanson, 1984; Murphy et al., 2021). In addition, ancient diamonds containing harzburgitic inclusion assemblages with suprachondritic initial $^{187}Os/^{188}Os$ ratios indicate growth in melt-depleted lithospheric mantle that had been metasomatized by hydrous carbon-bearing fluids (Westerlund et al., 2006). Despite these varied lines of evidence, the source of fluids and the mechanisms by which they were transported into the deep crust and lithospheric mantle are poorly understood.

On the modern Earth such mantle metasomatism occurs above subduction zones, where oceanic crust and overlying sediment are buried and heated, initiating dehydration reactions that release H_2O (and CO_2) and fluid-mobile trace elements into the surrounding mantle (Peacock, 1990), inducing partial melting. The pressure–temperature (P–T) conditions at which dehydration reactions occur are a function of the composition of the subducted material, but generally occur around the greenschist–amphibolite facies transition at temperatures of 350–500 °C for typical oceanic crustal materials (Peacock, 1990; Hacker et al., 2003). Accordingly, the evidence for fluid-mediated mantle metasomatism in the Archaean might suggest that subduction-like processes characterised by cold geotherms were in operation (Westerlund et al., 2006), such that dehydration could occur below the Moho (Foley et al., 2002). However, a paucity of evidence from the metamorphic rock record for geotherms characteristic of subduction processes before around 2.0 Ga (<500 °C.GPa^{-1}, Weller and St-Onge, 2017; Brown and Johnson, 2018) requires some other mechanism to transport fluids to upper mantle depths in the early Earth.

Variations in bulk-rock MgO content affect the abundance and stability of hydrous ferromagnesian silicate minerals, such as chlorite, serpentine and amphibole (Palin and White, 2016; Starr and Pattison, 2019). These minerals accommodate significant amounts of water as crystal-bound OH^-, such that variability in their modal abundance and stability profoundly affects the capacity of a given rock to retain water (Palin and White, 2016). Burial of hydrated ultramafic rocks in the lower crustal and lithospheric mantle portions of subducting slabs is a potentially important pathway for deep volatile recycling in modern subduction zones (van Keken et al., 2011). Nevertheless, the role of primitive mafic–ultramafic crust in the Archaean lithospheric water cycle has not been explored.

The generation of ultramafic magmas (MgO >18 wt%) formed by high-degree partial melting of mantle peridotite requires extreme temperatures (>1600 °C), consistent with an Archaean mantle that was significantly warmer than at present (Herzberg et al., 2007). Consequently, Archaean primary crust is characterised by

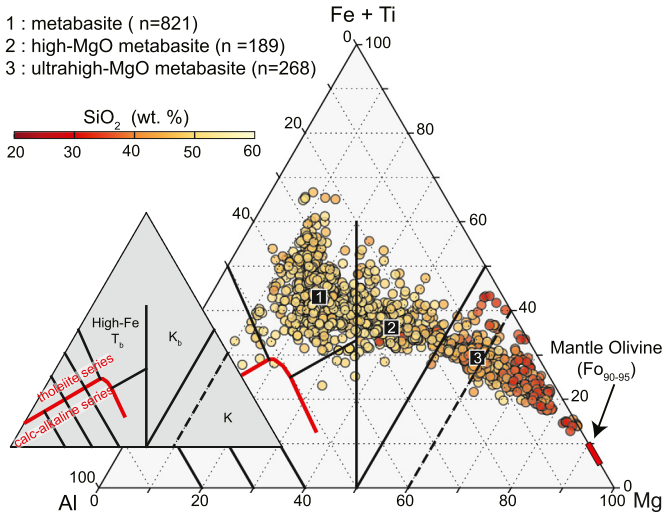

Fig. 1. Ternary classification diagram for sub-alkaline volcanic rocks illustrating the chemical variation in mafic-ultramafic volcanic rocks from the Yilgarn and Pilbara Cratons, Western Australia. The original komatiitic basalt (K_b)–komatiite (K) boundary (dashed black line) has been modified to better reflect natural compositional breaks based on classification using a total alkalis ($Na_2O + K_2O$) versus MgO diagram (Fig. S1). Numbered black squares (white font) denote the representative composition for each rock type used for thermodynamic modelling. (For interpretation of the colours in the figure(s), the reader is referred to the web version of this article.)

considerable variability in its MgO content (Fig. 1 and Fig. S1). At one extreme are komatiites, ultramafic (MgO >18 wt%) lavas that generally comprise about 2–5 percent by volume of exposed Archaean volcanic sequences, but which locally may be much more abundant (up to 30 vol.%, de Wit and Ashwal, 1995). In addition, Archaean greenstone sequences commonly contain high- and ultrahigh-MgO picrites, 'boninite-like' rocks, and ultramafic intrusive rocks such as pyroxenites and peridotites that formed by fractional crystallisation in mafic–ultramafic magmas (Szilas et al., 2015; Guice et al., 2018). The common development of pillow structures in many mafic and ultramafic rocks, along with oxygen isotopic and other geochemical data, indicates that the continents were almost entirely submerged in the Archaean (Flament et al., 2008; Johnson and Wing, 2020; Staude et al., 2020). The higher eruption temperatures and lower viscosities of ultramafic magmas means they were much more likely to have been erupted onto the Archaean seafloor and extensively hydrated (and silicified) during subsequent hydrothermal alteration (Dann, 2001; Kump and Barley, 2007, André et al., 2022).

Here, we present the results of phase equilibrium modelling of three representative mafic–ultramafic compositions (Fig. 1, Fig. S1, Tables S1 and S2), a metabasite (MgO ~7 wt% MgO), a high-MgO metabasite (~14 wt% MgO), and an ultrahigh-MgO metabasite (~25 wt% MgO), to investigate how MgO content affects the fluid budget of primary Archaean crust during prograde metamorphism. Ultrahigh-MgO metabasites are defined here as any extrusive or shallow crustal intrusive rocks with MgO >18 wt %, and include hydrated komatiites, ultrahigh-MgO picrites and boninite-like rocks, as well as pyroxenite and peridotite cumulates (e.g. Szilas et al., 2015). We show that the temperature at which major devolatilization occurs is positively correlated with protolith MgO content and that metamorphosed ultramafic rocks (MgO >18 wt%) undergo dehydration by chlorite breakdown at temperatures in excess of 700 °C. This means these rocks would have provided a key source of H_2O in the deep crust and/or lithospheric mantle in the early Earth.

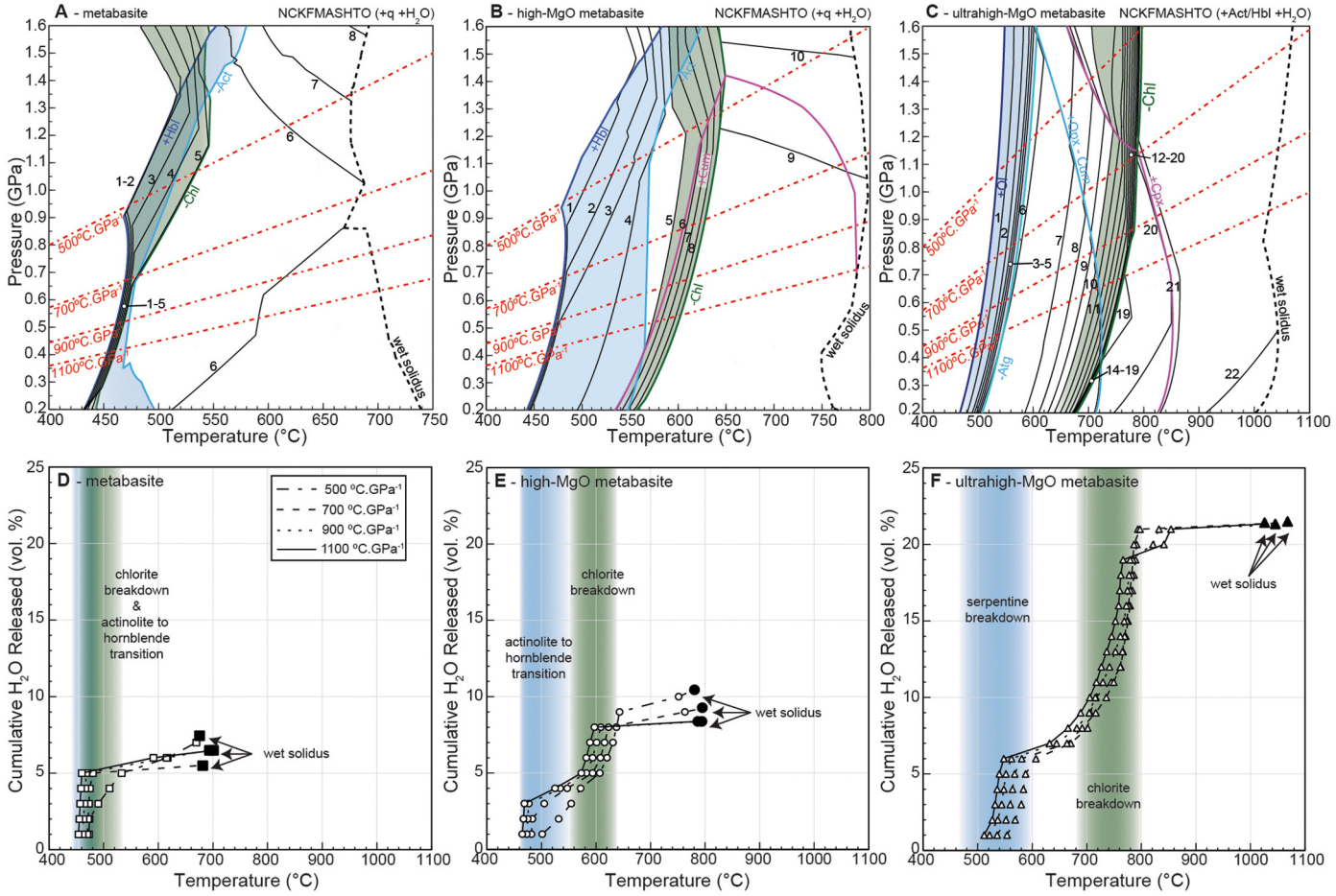

Fig. 2. A–C: Isochemical P–T pseudosections for representative samples of metabasite (**A**), high-MgO metabasite (**B**) and ultrahigh-MgO metabasite (**C**) protolith compositions. Coloured lines represent appearance and/or disappearance of major rock forming minerals. Solid black lines represent contours for cumulative amount of H_2O released at various P-T conditions. Dashed black lines denote the wet-solidi. Coloured fields highlight major dehydration intervals associated with actinolite-hornblende transition, serpentine breakdown (blue) and chlorite breakdown (green). **D–F**: Diagrams showing cumulative amount of H_2O released versus temperature along geothermal gradients ranging from 500 °C.GPa^{-1} to 1100 °C.GPa^{-1} for basaltic (**D**), picritic (**E**) and komatiitic (**F**) protoliths. In all rock types most water is released during chlorite breakdown, which occurs at increasingly higher temperatures (and thus pressure/depth) as the protolith MgO content increases.

2. Fluid budgets during burial and heating

Simplified isochemical *P–T* diagrams (pseudosections) for the three modelled compositions are shown in Figs. 2A–C, and include the (dis)appearance of key minerals along with contours for H_2O production (as mol.%, ~vol.%). Also shown are four geotherms ranging between 1100 and 500 °C.GPa^{-1}. The full phase diagrams are provided in the Supplementary Materials (Figs S2–4) along with details of their calculation. Curves showing the cumulative amount of H_2O released from each rock type with increasing temperature are shown in Fig. 2D–F. Changes in mineral modes in each rock type are depicted in modebox diagrams in Fig. S5.

Regardless of the geotherm, burial and heating of a typical fully-hydrated (seawater-altered) Archaean metabasite produces a maximum of around 5 vol.% H_2O. Most H_2O is produced across a narrow temperature interval between 450 and 510 °C corresponding to the breakdown of actinolite and chlorite to form hornblende (Fig. 2A, Fig. S2). Less than 1 vol.% H_2O is released with further increases in temperature (Fig. 2D) until the H_2O-saturated ('wet') solidus is reached at around 700 °C, at which point any free H_2O is consumed to form melt. For the high-MgO metabasite (Figs. 2B and 2E, Fig. S3), H_2O is mainly released in two dehydration steps. The first step, at 460–500 °C, is associated with the actinolite to hornblende transition to produce 3 vol.% H_2O. A second dehydration event is related to the breakdown of chlorite, the stability of which is extended to higher temperatures than in the basalt. The temperature interval over which chlorite breaks down is moderately pressure dependent, occurring at temperatures between 545 and 555 °C along a warm 1100 °C.GPa^{-1} geotherm, but between 610 and 650 °C along cooler geotherms (500 °C.GPa^{-1}). At temperatures above chlorite breakdown, there is negligible additional H_2O produced before reaching the H_2O-saturated solidus around 800 °C. Overall, the representative high-MgO metabasite produces some 8 vol.% H_2O, about 60% more H_2O than an equivalent volume of Archaean basaltic material.

The calculated phase equilibria for the ultrahigh-MgO metabasite (Figs. 2C and 2F, Fig. S4) shows some important differences from the other compositions. At lower temperatures, antigorite (serpentine) is stable, and its breakdown to form olivine marks the first major dehydration event, which liberates around 6 vol.% H_2O between 480 and 600 °C. However, chlorite breakdown occurs at much higher temperatures of between 700 and 800 °C, releasing a large volume of H_2O (around 14–16 vol.%). Thus, ultrahigh-MgO metabasites can store then liberate around four times as much H_2O as an equivalent volume of Archaean low-MgO metabasite, most of which is released at substantially higher temperature (Fig. 2F). Although the presence of CO_2 from devolatilising carbonate within mafic–ultramafic rocks affects the phase equilibria (Elmer et al., 2006; Powell et al., 1991), CO_2 plays an insignificant role in the temperatures of antigorite and chlorite breakdown for plausible quantities of carbonate within the protolith (Fig. S6).

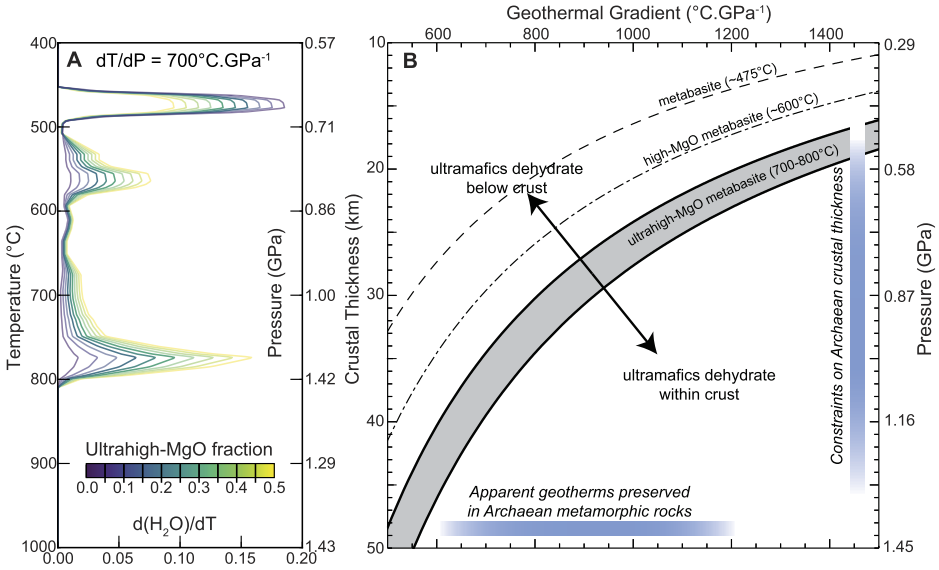

Fig. 3. A. Modelled fluid production versus temperature curves with variable proportions of ultrahigh-MgO material. Note that increasing ultramafic rocks fractions increase the proportion of fluid released at high-temperature. **B**. Plot of Archaean geotherms versus crustal thickness with isotherms corresponding to the approximate temperature of chlorite breakdown reactions in each end-member rock type, depicting the depths at which dehydration will occur in the basaltic, picritic and komatiitic (grey field) protoliths along a given geotherm.

3. Consequences for volatile recycling in the early Earth

On modern Earth, the upper (basaltic) levels of oceanic crust show limited variability in MgO content (mainly 7–9 wt%) (White et al., 2014), and dehydration reactions occur over a restricted temperature range (350–500 °C) (Hacker et al., 2003). By contrast, our phase equilibrium modelling indicates that, on burial and heating, metamorphic fluids would have been released from compositionally-variable Archaean mafic–ultramafic crust over a much wider range of temperatures and pressures/depths (Fig. 2).

Whether release of hydrous fluids occurs within the crust or the lithospheric mantle is a function of the composition of the crust being buried, the thickness of the crust and the geotherm (Fig. 3A, Figs. S7 and S8). The thickness of primary mafic–ultramafic crust is positively correlated with mantle temperature (Herzberg et al., 2010). Although the temperature of the upper mantle in the early Archaean is debated (Herzberg et al., 2010; Ganne and Feng, 2017), most estimates suggest mantle potential temperature was at least 150 °C warmer than the present day, and that primary crustal thicknesses were 20–45 km (Herzberg et al., 2010). These results are consistent with the trace element composition of most TTG that formed by intracrustal melting of amphibolite in the stability field of garnet, requiring a crustal thickness of at least ~20–25 km assuming an average density of 2950 kg.m^{-3} (Bédard, 2006; Johnson et al., 2017). Phase equilibrium calculations suggest most TTG formed under crustal geotherms of 700 °C.GPa^{-1} or higher (Johnson et al., 2017), consistent with the range of apparent geotherms estimated from the metamorphic rock record (600–1200 °C.GPa^{-1}) (Brown and Johnson, 2018).

Assuming a minimum thickness of 20 km for early Archaean mafic–ultramafic crust, typical Archaean hydrated metabasites would have undergone major dehydration within the crust for geotherms greater than around 800 °C.GPa^{-1} (Fig. 3B). Importantly, at a crustal thickness of 20 km and for all plausible geotherms (<1100–1200 °C.GPa^{-1}), both high-MgO metabasites and ultrahigh-MgO metabasites would have undergone chlorite dehydration at depths below the Moho (Fig. 3B), leading to hydration and enrichment of the lithospheric mantle in fluid-mobile elements, and promoting partial melting of that source to produce enriched basalts.

For a crustal thickness of 30 km and geotherms >700 °C.GPa^{-1}, major pulses of intracrustal dehydration by breakdown of chlorite in metabasite and high-MgO metabasite, and of antigorite in ultrahigh-MgO metabasite, release H_2O to hydrate overlying dry or H_2O-undersaturated mafic rocks, making them more fertile to subsequent partial melting when buried to deeper crustal levels. If fluid produced by dehydration of less magnesium rocks in the mid crust was not highly channelised, adjacent ultramafic intrusions would potentially have become hydrated, and would have acted as a 'sponge', permitting transportation of H_2O to much greater, rather than lesser, depths (Fig. 3A). Under these conditions, chlorite dehydration in ultrahigh-MgO metabasite may still have occurred within the lithospheric mantle for a geotherm <900 °C.GPa^{-1} (Fig. 3B). By contrast, for crust >40 km thick and plausible geotherms (>600 °C.GPa^{-1}), dehydration of all modelled lithologies would have occurred within the crust. Chlorite breakdown in ultrahigh-MgO metabasite occurs at temperatures above the H_2O-saturated-solidi for Archaean metabasite and high-MgO metabasite (Fig. 3), but not above the solidi for strongly H_2O-undersaturated intrusive equivalents.

Subduction buries upper crustal rocks along cool geotherms (Peacock, 1990), providing an ideal mechanism for transporting fluids into the mantle. Indeed, many greenstone sequences throughout the Archaean eon contain enriched and hydrated 'boninite-like' magmas similar to those that characterise the initiation stages of modern subduction zones (Smithies et al., 2018), where strongly-depleted mantle is fluxed by trace-element enriched 'crustal' fluids. The occurrence of 'boninite-like' rocks in many greenstone belts could reflect partial melting of lithospheric mantle due to high-temperature dehydration of ultramafic rocks buried in 'warm' Archaean subduction zones (Fig. 4A). However, even more common in Archaean sequences are high-Mg basaltic rocks that preserve variolitic textures believed to reflect fluid-fluxed melting of lithospheric mantle (Murphy et al., 2021). In the eastern Pilbara Craton in Western Australia, these voluminous variolitic basalts are included among the oldest preserved volcanic rocks in the region (3.47 billion years old), and are argued to have formed in a stagnant-lid regime (Murphy et al., 2021). Numerical modelling has shown intraplate 'sagduction' processes are also able to bury hydrated upper crustal rocks to upper mantle depths

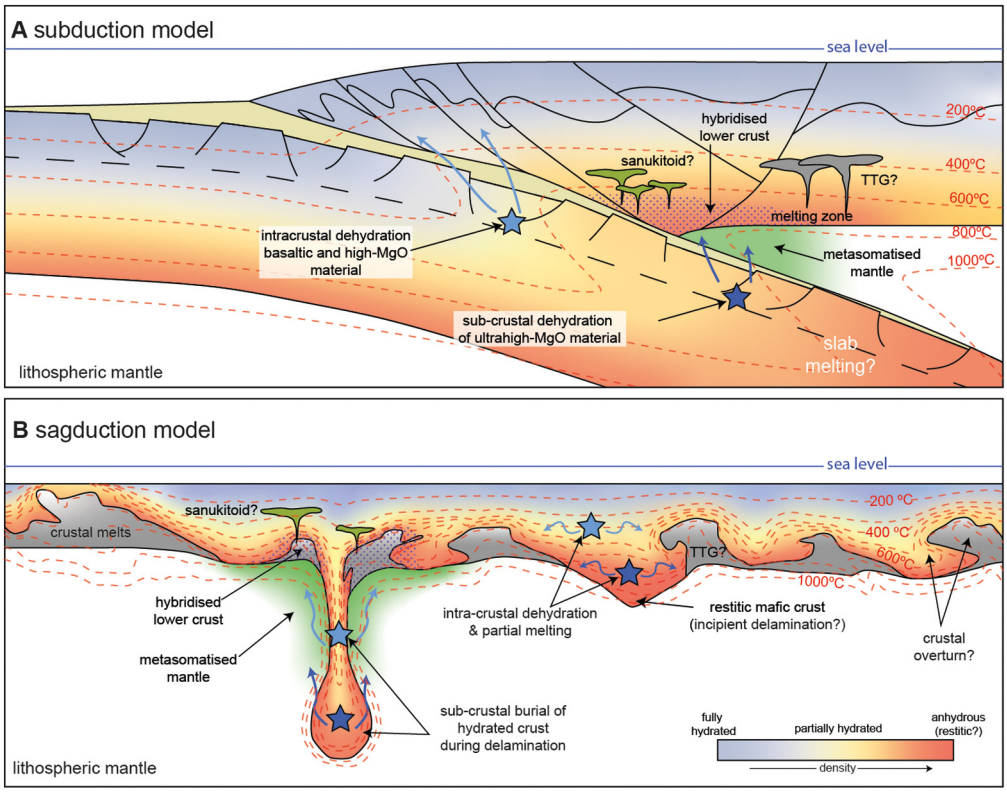

Fig. 4. Schematic diagrams showing plausible end-member scenarios. **A**. A warm Archaean subduction zone shows mantle metasomatism and TTG formation occurring above a dehydrating slab. **B**. TTG generation by fluid-fluxed melting of mafic crust in an intraplate setting, modified after numerical models from Sizova et al., 2015.

along geotherms similar to those that characterise hot subduction zones (Sizova et al., 2015). Given the ability of hydrated mafic–ultramafic volcanic rocks to transport volatiles to depth under geotherms $>500\,^{\circ}C.GPa^{-1}$ suggests that subduction-like environments may not have been required. Instead, these volatiles could have been transported into the mantle via sinking greenstone drips (Fig. 4B; Bédard, 2006; Johnson et al., 2016; Murphy et al., 2021; Smithies et al., 2021).

4. Implications for the generation of TTG magmas

The presence of hydrous fluids lowers the melting temperature of metabasalt to 650–700 °C. Fluid-fluxed melting produces TTG melts with 'high-pressure' trace element signatures (high-Sr and low-HREE contents), in which the volume of melt produced is proportional to the volume of external fluid added until the melt becomes saturated in H_2O (Pourteau et al., 2020). The presence of a significant fluid reservoir in the lower portions of Archaean primary mafic-ultramafic crust obviates the need for inverted thermal gradients to introduce fluids at temperatures conducive to partial melting (Clemens et al., 2020). Instead, the formation of significant volumes of TTG magma in the lower parts of primary Archaean crust may have been an inevitable consequence of magmatic thickening of variably hydrated ultramafic-rich crust along warm Archaean geotherms (e.g. Webb et al., 2020).

Modelling of the bulk Archaean crustal fluid budgets clearly shows that the dehydration and subsequent partial melting of primary mafic-ultramafic crust is sensitive to the proportion of hydrated ultramafic rock present (Fig. 3A). For ultramafic rock abundances of 30%, comparable to some komatiite-rich greenstone belts (de Wit and Ashwal, 1995) or greenstone belts with abundant MgO-rich boninite-like rocks and ultramafic intrusions such as Isua in West Greenland (Furnes et al., 2009; Szilas et al., 2015), the total fluid budget of Archaean crust is twice that of crust comprising only metabasite (Fig. 3A, Fig. S7 and S8). Importantly, in crust with 30% ultramafic rocks, >50% of this fluid is released at temperatures >700 °C. For ultramafic rock contents of 5%, comparable to the average abundance of komatiite in greenstone belts (de Wit and Ashwal, 1995), the fluid carrying capacity of Archaean crust increases by 20% (Figs. S7 and S8), 17% of which is released at temperatures >700 °C. In addition to hydration, silicification (metasomatism) during seafloor alteration of Archean primary crust was likely important in decreasing solidus temperatures and/or increasing melt fertility (André et al., 2019, 2022), with each mole of quartz at the solidus yielding approximately 2 moles of melt upon heating to 850 °C (Stuck and Diener, 2017). In regions dominated by cooler geothermal gradients, where fluids locked within the ultramafic component of Archaean crust were released within the lithospheric mantle, TTGs may have formed by a two-stage process. The release of fluids in the lithospheric mantle would have promoted partial melting and advection of enriched hydrous mafic magmas into the lower crust (Fig. 4), contributing additional heat and fluids to form the hybridised mafic source of TTG (Smithies et al., 2021).

These results therefore highlight that the differentiation of Earth's primary mafic–ultramafic crust likely proceeded by a combination of processes, including both fluid-absent and fluid-present crustal anatexis, to produce TTG of variable compositions; where the extent of fluid-present melting, and the formation of seemingly 'high-pressure' (high Sr/Y) TTG, was limited by the availability of free water supplied by hydrated lower crustal ultramafic material. Fluid-present melting models may not fully account for crustal differentiation throughout the Archaean, but should be more widely applicable to the earliest felsic Hadean-Eoarchaean proto-continents which are believed to have formed above regions of anomalously hot mantle via partial melting of primary mafic–ultramafic crust that was subject to hydrothermal alteration (Reimink et al., 2014; André et al., 2019, 2022). Given the strong

dependence of melt productivity with the volume of external fluid supplied to sustain fluid-present melting (Pourteau et al., 2020), an intriguing and counter-intuitive implication of our model is that the development of Earth's proto-continents in the early Archaean might reflect a primordial variability in the proportion of ultramafic rock (and water content) of Earth's primary mafic–ultramafic crust.

Evidence for these processes in the rock record may be preserved in the Lewisian Complex in NW Scotland, where amphibole-bearing metaperidotites and metapyroxenites are interlayered with garnet-bearing metabasic migmatites (Guice et al., 2018). These rocks show a close spatial and temporal association with garnet-biotite gneisses interpreted to be of (volcano) sedimentary origin (Johnson et al., 2016). The metaperidotites have a similar mineralogy to those predicted for hydrated komatiites metamorphosed to granulite facies (Fig. S4), and these lithological associations have been interpreted by some to represent an Archaean greenstone sequence that sunk into the lower crust (Johnson et al., 2016). Moreover, the greenstone sequence at Isua in West Greenland, preserves a range of mafic–ultramafic rocks types, including metabasic rocks containing Mg-rich chlorite (Furnes et al., 2009) and amphibole-bearing olivine serpentinites (Szilas et al., 2015), both of which are indicative of hydrated ultramafic protoliths.

5. Conclusions

Throughout the Archaean, Earth was covered in a global ocean (Bindeman et al., 2018), such that most or all mafic and ultramafic lavas were erupted under water. The recognition that hydrated ultramafic rocks dehydrate at elevated temperatures highlights a new geochemical pathway for recycling of volatiles into the deep crust and upper mantle on a hotter early Earth. Depending on local crustal composition and thickness, and the ambient conductive geotherm, high-temperature dehydration of ultramafic rocks such as, but not limited to, komatiite, would have caused hydration and/or fluid-present melting of overlying lower MgO rock types, ultimately to form TTG magmas, the building blocks of ancient continental crust. Alternatively, if liberated at subcrustal depths, such fluids would have metasomatized the lithospheric mantle to form the source of enriched Archaean basalts.

6. Methods

Methods and any associated references are available in the supplementary information provided.

CRediT authorship contribution statement

Michael I.H. Hartnady: Conceptualization, Investigation, Methodology, Visualization, Writing – review & editing. **Tim E. Johnson:** Conceptualization, Investigation, Methodology, Validation, Writing – review & editing. **Simon Schorn:** Conceptualization, Investigation, Methodology, Writing – review & editing. **R. Hugh Smithies:** Conceptualization, Investigation, Validation, Writing – review & editing. **Christopher L. Kirkland:** Validation, Writing – review & editing. **Stephen H. Richardson:** Validation, Writing – review & editing.

Declaration of competing interest

The authors declare that they have no known competing financial interests or personal relationships that could have appeared to influence the work reported in this paper

Data and materials availability

All data used in this study are available in the main text and in the supplementary materials. The software and datafiles used to generate the phase diagrams presented herein can be downloaded at http://www.metamorph.geo.uni-mainz.de/thermocalc.

Acknowledgements

This research was supported by an Australian Research Council (ARC) grant LP180100199 in conjunction with Northern Star Resource Ltd and the Geological Survey of Western Australia. T.E.J. acknowledges funding from the Australian Government through an Australian Research Council Discovery Project (DP200101104), and support from the State Key Laboratory for Geological Processes and Mineral Resources, China University of Geosciences, Wuhan (Open Fund GPMR202101). S.S. acknowledges support from an Austrian Science Fund (FWF) grant P-33002-N (SS). We are grateful to Luc André and an anonymous reviewer whose comments led to significant improvements in the paper, and to Mike Brown who's comments on an earlier version of this work helped to clarify our arguments. Frederic Moynier is thanked for efficient editorial handling. R.H.S. publishes with the permission of the Executive Director, Geological Survey of Western Australia.

Appendix A. Supplementary material

Supplementary material related to this article can be found online at https://doi.org/10.1016/j.epsl.2022.117695.

References

André, L., Abraham, K., Hofmann, A., Monin, L., Kleinhanns, I.C., Foley, S., 2019. Early continental crust generated by reworking of basalts variably silicified by seawater. Nat. Geosci. 12, 769–773.

André, L., Monin, L., Hofmann, A., 2022. The origin of early continental crust: new clues from coupling Ge/Si ratios with silicon isotopes. Earth Planet. Sci. Lett. 582, 117415.

Barker, F., Arth, J.G., 1976. Generation of trondhjemitic-tonalitic liquids and Archean bimodal trondhjemite-basalt suites. Geology 4, 596–600.

Bindeman, I., Zakharov, D., Palandri, J., Greber, N.D., Dauphas, N., Retallack, G., Hofmann, A., Lackey, J., Bekker, A., 2018. Rapid emergence of subaerial landmasses and onset of a modern hydrologic cycle 2.5 billion years ago. Nature 557, 545–548.

Brown, M., Johnson, T.E., 2018. Secular change in metamorphism and the onset of global plate tectonics. Am. Mineral. 103, 181–196.

Byerly, B.L., Kareem, K., Bao, H., Byerly, G.R., 2017. Early Earth mantle heterogeneity revealed by light oxygen isotopes of Archaean komatiites. Nat. Geosci. 10, 871–875.

Bédard, J.H., 2006. A catalytic delamination-driven model for coupled genesis of Archaean crust and sub-continental lithospheric mantle. Geochim. Cosmochim. Acta 70, 1188–1214.

Clemens, J.D., Stevens, G., Bryan, S.E., 2020. Conditions during the formation of granitic magmas by crustal melting–hot or cold; drenched, damp or dry? Earth-Sci. Rev. 200, 102982.

Dann, J.C., 2001. Vesicular komatiites, 3.5-Ga Komati Formation, Barberton Greenstone Belt, South Africa: inflation of submarine lavas and origin of spinifex zones. Bull. Volcanol. 63, 462–481.

de Wit, M.J., Ashwal, L.D., 1995. Greenstone belts: what are they? S. Afr. J. Geol. 98, 505–520.

Elmer, F., White, R., Powell, R., 2006. Devolatilization of metabasic rocks during greenschist–amphibolite facies metamorphism. J. Metamorph. Geol. 24, 497–513.

Flament, N., Coltice, N., Rey, P.F., 2008. A case for late-Archaean continental emergence from thermal evolution models and hypsometry. Earth Planet. Sci. Lett. 275, 326–336.

Foley, S., Tiepolo, M., Vannucci, R., 2002. Growth of early continental crust controlled by melting of amphibolite in subduction zones. Nature 417, 837–840.

Furnes, H., Rosing, M., Dilek, Y., de Wit, M., 2009. Isua supracrustal belt (Greenland)—a vestige of a 3.8 Ga suprasubduction zone ophiolite, and the implications for Archean geology. Lithos 113, 115–132.

Ganne, J., Feng, X., 2017. Primary magmas and mantle temperatures through time. Geochem. Geophys. Geosyst. 18, 872–888.

Guice, G.L., McDonald, I., Hughes, H.S., MacDonald, J.M., Blenkinsop, T.G., Goodenough, K.M., Faithfull, J.W., Gooday, R.J., 2018. Re-evaluating ambiguous age relationships in Archean cratons: implications for the origin of ultramafic-mafic complexes in the Lewisian Gneiss Complex. Precambrian Res. 311, 136–156.

Hacker, B.R., Peacock, S.M., Abers, G.A., Holloway, S.D., 2003. Subduction factory 2. Are intermediate-depth earthquakes in subducting slabs linked to metamorphic dehydration reactions? J. Geophys. Res., Solid Earth 108 (B1).

Herzberg, C., Asimow, P.D., Arndt, N., Niu, Y., Lesher, C., Fitton, J., Cheadle, M., Saunders, A., 2007. Temperatures in ambient mantle and plumes: constraints from basalts, picrites, and komatiites. Geochem. Geophys. Geosyst. 8, Q02006.

Herzberg, C., Condie, K., Korenaga, J., 2010. Thermal history of the Earth and its petrological expression. Earth Planet. Sci. Lett. 292, 79–88.

Johnson, B.W., Wing, B.A., 2020. Limited Archaean continental emergence reflected in an early Archaean 18 O-enriched ocean. Nat. Geosci. 13, 243–248.

Johnson, T.E., Brown, M., Gardiner, N.J., Kirkland, C.L., Smithies, R.H., 2017. Earth's first stable continents did not form by subduction. Nature 543, 239–242.

Johnson, T.E., Brown, M., Goodenough, K.M., Clark, C., Kinny, P.D., White, R.W., 2016. Subduction or sagduction? Ambiguity in constraining the origin of ultramafic–mafic bodies in the Archean crust of NW Scotland. Precambrian Res. 283, 89–105.

Kleinhanns, I.C., Kramers, J.D., Kamber, B.S., 2003. Importance of water for Archaean granitoid petrology: a comparative study of TTG and potassic granitoids from Barberton Mountain Land, South Africa. Contrib. Mineral. Petrol. 145, 377–389.

Kump, L.R., Barley, M.E., 2007. Increased subaerial volcanism and the rise of atmospheric oxygen 2.5 billion years ago. Nature 448, 1033–1036.

Liou, P., Wang, Z., Mitchell, R.N., Doucet, L.S., Li, M., Guo, J., Zhai, M., 2022. Fe isotopic evidence that "high pressure" TTGs formed at low pressure. Earth Planet. Sci. Lett. 592, 117645.

Moyen, J.-F., 2011. The composite Archaean grey gneisses: petrological significance, and evidence for a non-unique tectonic setting for Archaean crustal growth. Lithos 123, 21–36.

Moyen, J.-F., Stevens, G., 2006. Experimental constraints on TTG petrogenesis: implications for Archean geodynamics. In: Benn, K., Mareschal, J.-C., Condie, K.C. (Eds.), Archean Geodynamics and Environments. In: Geophysical Monograph Series, vol. 164, pp. 149–175.

Murphy, D.T., Wiemer, D., Bennett, V.C., Spring, T., Trofimovs, J., Cathey, H.E., 2021. Paleoarchean variole-bearing metabasalts from the East Pilbara Terrane formed by hydrous fluid phase exsolution and implications for Archean greenstone belt magmatic processes. Precambrian Res. 357, 106114.

Palin, R.M., White, R.W., 2016. Emergence of blueschists on Earth linked to secular changes in oceanic crust composition. Nat. Geosci. 9, 60–64.

Peacock, S.A., 1990. Fluid processes in subduction zones. Science 248, 329–337.

Pourteau, A., Doucet, L.S., Blereau, E.R., Volante, S., Johnson, T.E., Collins, W.J., Li, Z.-X., Champion, D.C., 2020. TTG generation by fluid-fluxed crustal melting: direct evidence from the Proterozoic Georgetown Inlier, NE Australia. Earth Planet. Sci. Lett. 550, 116548.

Powell, R., Will, T., Phillips, G., 1991. Metamorphism in Archaean greenstone belts: calculated fluid compositions and implications for gold mineralization. J. Metamorph. Geol. 9, 141–150.

Reimink, J.R., Chacko, T., Stern, R.A., Heaman, L.M., 2014. Earth's earliest evolved crust generated in an Iceland-like setting. Nat. Geosci. 7, 529–533.

Shirey, S.B., Hanson, G.N., 1984. Mantle-derived Archaean monozodiorites and trachyandesites. Nature 310, 222–224.

Sizova, E., Gerya, T., Stüwe, K., Brown, M., 2015. Generation of felsic crust in the Archean: a geodynamic modeling perspective. Precambrian Res. 271, 198–224.

Smithies, R.H., 2002. Archaean boninite-like rocks in an intracratonic setting. Earth Planet. Sci. Lett. 197, 19–34.

Smithies, R.H., Champion, D., Van Kranendonk, M.J., 2009. Formation of Paleoarchean continental crust through infracrustal melting of enriched basalt. Earth Planet. Sci. Lett. 281, 298–306.

Smithies, R.H., Ivanic, T.J., Lowrey, J.R., Morris, P.A., Barnes, S.J., Wyche, S., Lu, Y.-J., 2018. Two distinct origins for Archean greenstone belts. Earth Planet. Sci. Lett. 487, 106–116.

Smithies, R.H., Lu, Y., Kirkland, C.L., Johnson, T.E., Mole, D.R., Champion, D.C., Martin, L., Jeon, H., Wingate, M.T., Johnson, S.P., 2021. Oxygen isotopes trace the origins of Earth's earliest continental crust. Nature 592, 70–75.

Sobolev, A.V., Asafov, E.V., Gurenko, A.A., Arndt, N.T., Batanova, V.G., Portnyagin, M.V., Garbe-Schönberg, D., Wilson, A.H., Byerly, G.R., 2019. Deep hydrous mantle reservoir provides evidence for crustal recycling before 3.3 billion years ago. Nature 571, 555–559.

Starr, P.G., Pattison, D.R., 2019. Metamorphic devolatilization of basalts across the greenschist-amphibolite facies transition zone: insights from isograd mapping, petrography and thermodynamic modelling. Lithos 342, 295–314.

Staude, S., Jones, T.J., Markl, G., 2020. The textures, formation and dynamics of rare high-MgO komatiite pillow lavas. Precambrian Res. 343, 105729.

Stuck, T.J., Diener, J.F.A., 2017. Mineral equilibria constrains on open-system melting in metamafic compositions. J. Metamorph. Geol. 36, 255–281.

Szilas, K., Kelemen, P.B., Rosing, M.T., 2015. The petrogenesis of ultramafic rocks in the >3.7 Ga Isua supracrustal belt, southern West Greenland: geochemical evidence for two distinct magmatic cumulate trends. Gondwana Res. 28, 565–580.

van Keken, P.E., Hacker, B.R., Syracuse, E.M., Abers, G.A., 2011. Subduction factory: 4. Depth-dependent flux of H_2O from subducting slabs worldwide. J. Geophys. Res., Solid Earth 116 (B1).

Webb, A.A.G., Müller, T., Zuo, J., Haproff, P.J., Ramírez-Salazar, A., 2020. A non–plate tectonic model for the Eoarchean Isua supracrustal belt. Lithosphere 12, 166–179.

Weller, O., St-Onge, M., 2017. Record of modern-style plate tectonics in the Palaeoproterozoic Trans-Hudson orogen. Nat. Geosci. 10, 305–311.

Westerlund, K., Shirey, S., Richardson, S., Carlson, R., Gurney, J., Harris, J., 2006. A subduction wedge origin for Paleoarchean peridotitic diamonds and harzburgites from the Panda kimberlite, Slave craton: evidence from Re–Os isotope systematics. Contrib. Mineral. Petrol. 152, 275–294.

White, W., Klein, E., Holland, H., Turekian, K., 2014. Composition of the oceanic crust. In: Holland, H.D., Turekian, K.K. (Eds.), Treatise on Geochemistry, second ed. Elsevier, Oxford, pp. 457–496.